Nano Research

ISSN 1998-0124 CN 11-5974/O4
https://doi.org/10.26599/NR.2026.94909226

Research Article

Atmosphere and temperature regulated fluorescence intermittency of carbon dots from single-particle dynamics to ensemble photostability

Zhihong Wei[1,2,§], Yixin Ouyang[2,§], Juan Chen[1], Jingtao Huang[1], Denghui Liu[1], Yiru Jiang[1], Sen Luo[2], Boyang Wang[3], Wei Li[1], Siyu Lu[3](✉), Yuxi Tian[2](✉)

[1] Department of Forensic Science and Technology, Zhengzhou Police University, Zhengzhou 450000, China

[2] State Key Laboratory of Analytical Chemistry for Life Science, Key Laboratory of Mesoscopic Chemistry of MOE, School of Chemistry, Nanjing University, Nanjing 210023, China

[3] Green Catalysis Center, and College of Chemistry, Zhengzhou University, Zhengzhou 450000, China

[§] Zhihong Wei, and Yixin Ouyang contributed equally to this work.

Nano Res., **Just Accepted Manuscript** • https://doi.org/10.26599/NR.2026.94909226

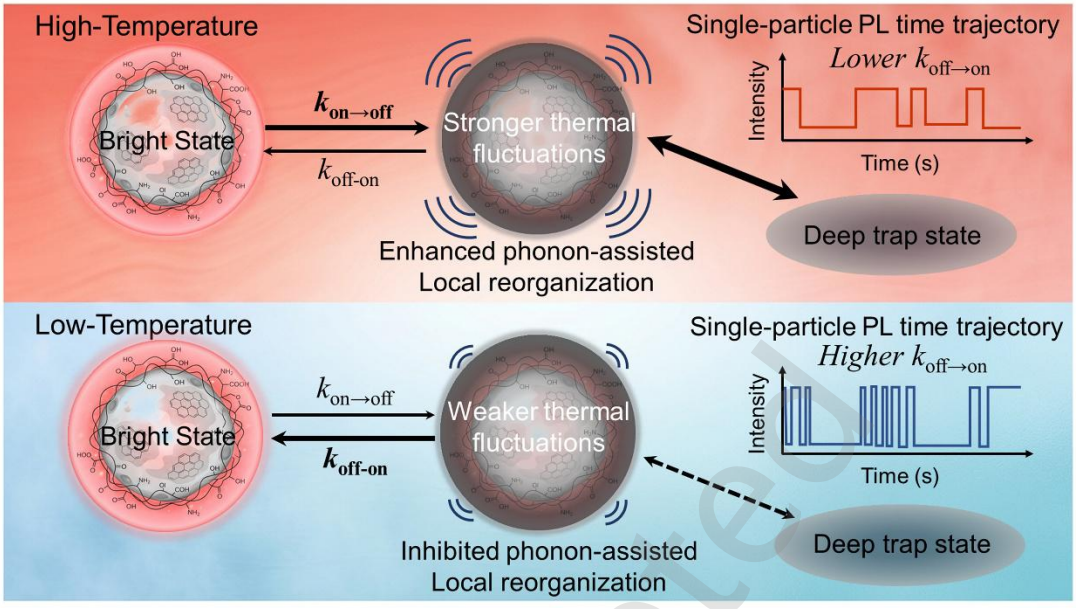
https://www.sciopen.com/journal/1998-0124 on Sep. 28, 2026

© The Authors(s)

Just Accepted

This is a "Just Accepted" manuscript, which has been examined by the peer-review process and has been accepted for publication. A "Just Accepted" manuscript is published online shortly after its acceptance,which is prior to technical editing and formatting and author proofing. Tsinghua University Press (TUP) provides "Just Accepted" as an optional and free service which allows authors to make their results available to the research community as soon as possible after acceptance. After a manuscript has been technically edited and formatted, and the page proofs have been corrected, it will be removed from the "Just Accepted" web site and published officially with volume and article number (e.g., *Nano Research*, **2025**, *18*, 94906990). Please note that technical editing may introduce minor changes to the manuscript text and/or graphics which may affect the content, and all legal disclaimers that apply to the journal pertain. In no event shall TUP be held responsible for errors or consequences arising from the use of any information contained in these "Just Accepted" manuscripts. To cite this anuscript please use its Digital Object Identifier (DOI®),which is identical for all formats of publication.

TABLE OF CONTENTS (TOC)



Atmosphere and temperature modulate carbon dot fluorescence by controlling the transition between emissive and non-emissive states, establishing the relationship between microscopic blinking dynamics and macroscopic photostability.

Just Accepted

Nano Research

Open Access

Research Article

Atmosphere and temperature regulated fluorescence intermittency of carbon dots from single-particle dynamics to ensemble photostability

Zhihong Wei[1,2,§], Yixin Ouyang[2,§], Juan Chen[1], Jingtao Huang[1], Denghui Liu[1], Yiru Jiang[1], Sen Luo[2], Boyang Wang[3], Wei, Li[1], Siyu Lu[3,✉], and Yuxi Tian[2,✉]

[1] *Department of Forensic Science and Technology, Zhengzhou Police University, Zhengzhou 450000, China*
[2] *State Key Laboratory of Analytical Chemistry for Life Science, Key Laboratory of Mesoscopic Chemistry of MOE, School of Chemistry, Nanjing University, Nanjing 210023, China*
[3] *Green Catalysis Center, and College of Chemistry, Zhengzhou University, Zhengzhou 450000, China*

Received: 28 July 2026; **Revised:** 10 September 2026; **Accepted:** 28 September 2026

✉Address correspondence to Yuxi Tian, tyx@nju.edu.cn; Siyu Lu, sylu2013@zzu.edu.cn

Cite this article: *Nano Research*, 2026, 19, 94909226 https://doi.org/10.26599/NR.2026.94909226

ABSTRACT: Fluorescence instability of carbon dots (CDs) under continuous excitation originates from heterogeneous surface-state dynamics but remains poorly understood. Here, we combine ensemble fluorescence measurements with single-particle analysis to investigate how atmosphere and temperature regulate the fluorescence intermittency and photostability of CDs. Correlative ensemble and single-particle analyses demonstrate that oxygen-induced instability originates from increased occupation of long-lived dark states and irreversible loss of emissive centers. Conversely, decreasing the temperature enhances fluorescence stability by increasing the reversibility of dark states rather than simply suppressing their formation. The accelerated off-to-on recovery at reduced temperature decreases the accumulation of persistent non-emissive populations and consequently increases emissive-state occupancy under continuous excitation. These findings reveal that CDs photostability is determined by the dynamic regulation of emissive-state switching under environmental perturbations. This mechanistic insight provides guidance for designing CDs with optimized surface states and enhanced fluorescence stability.

KEYWORDS: carbon dots; single-particle spectroscopy; fluorescence intermittency; photostability

Just Accepted

Introduction

Carbon dots (CDs) have emerged as a versatile class of photoluminescent carbon nanomaterials for bioimaging, fluorescence sensing, and solid-state emission technologies, where long-term brightness stability often matters more than a one-time peak quantum yield (QY)[1-3]. Under continuous excitation and typically ambient operation in air, however, CDs commonly exhibit pronounced intensity decay, which compromises quantitative accuracy (e.g., long-term tracking or ratio-metric sensing) and accelerates devices degradation[4-6]. Crucially, ensemble stability metrics (photobleaching curves, average lifetimes, or bulk intensity changes) do not necessarily reflect a homogeneous material response; instead, they represent a statistical convolution of many nonidentical emissive centers that may undergo reversible blinking, transient quenching, and irreversible photochemical loss[7-9]. Disentangling these microscopic pathways therefore requires single-particle measurements that resolve when an emitter enters a dark state, how it recovers, and when it is permanently lost.

Single-emitter fluorescence intermittency has been extensively explored in both organic dye molecules and semiconductor quantum dots (SQDs). In single dye molecules, intensity fluctuations typically arise from transitions among metastable dark states or photoinduced reactions, most commonly intersystem crossing into the long-lived triplet, formation of radical states via electron transfer, reversible isomerization, and slow rearrangements of molecular conformation or the local nano-environment[10-12]. In contrast, blinking in SQDs is often characterized by broad distributions of on- and off-times that can extend over a wide temporal range and commonly follow power-law statistics. This behavior is generally linked to carrier trapping and charging/discharging processes, in which photoexcited carriers are transferred to surface or environmental trap states and the charged emitters are subsequently quenched through nonradiative pathways[13-15]. Blinking mechanisms identified for single molecules and SQDs provide useful conceptual reference points for understanding CDs. However, these models cannot be directly applied to CDs, because CDs typically contain structurally heterogeneous carbonized cores, diverse surface functional groups, and strongly environment-dependent energy dissipation pathways.

The structure of CDs is inherently imperfect, influenced by factors such as defects, heteroatom doping, and the finite size of sp^2 domains[16,17]. As a result, they do not possess a single well-defined emissive level; instead, a manifold of emissive and trap states emerges, with strong interfacial coupling[18]. Consequently, the competition between radiative recombination and nonradiative decay pathways is highly sensitive to subtle variations in the local chemical and thermal environment. Changes in pH or ionic strength can protonate/deprotonate surface groups and reorganize the hydrogen-bonding network,

thereby shifting surface-state energies and modulating charge-transfer barriers[19-21]; atmospheric components, especially O_2 , can act as an efficient electron acceptor and promote reversible quenching via charge separation as well as irreversible photo-oxidation; and temperature can tune phonon-assisted relaxation, trap escape, and thermally activated structural fluctuations that govern the accessibility, lifetime, and reversibility of dark states[22,23]. Under continuous excitation, these environment-dependent processes can manifest as altered on/off statistics, modified blinking amplitude and recovery probability, and different rates of permanent photochemical loss, which ultimately determines how single-emitter intermittency translates into ensemble photostability. Therefore, systematically clarifying how atmosphere and temperature reshape single-particle blinking kinetics is essential for disentangling reversible intermittency from irreversible degradation and for reliably deploying CDs under typical ambient operating conditions.

In this work, ensemble fluorescence measurements were combined with single-particle analyses to investigate how atmosphere and temperature influence the fluorescence intermittency and photostability of carbon dots (CDs). These experiments further reveal how single-particle dynamics are manifested in ensemble photobleaching behavior. We show that oxygen strongly promotes long-lived non-emissive states and increases the probability of irreversible loss of PL, whereas lowering temperature increases emissive-state occupancy mainly by enhancing the reversibility of dark states. These results establish a direct link between heterogeneous single-particle kinetics and macroscopic photostability, and provide a mechanistic basis for understanding and improving the operational stability of carbon dots under ambient conditions.

Results and discussion

Atmosphere strongly affects the ensemble photobleaching kinetics of R-CDs under continuous excitation (Fig. 1 and Fig. S1). Ensemble photobleaching traces were recorded in N_2 and O_2 atmospheres. In N_2 , the normalized photoluminescence (PL) intensity decays only slightly over 300 s and levels off at ≈0.59 of the initial value, indicating that a large fraction of emitters remain active within the observation window. By contrast, in O_2 the PL intensity drops rapidly during the first tens of seconds and approaches a low plateau of ≈0.18, evidencing pronounced oxygen-accelerated bleaching. The behavior observed in air closely mirrors that in O_2. To quantify the bleaching kinetics, the ensemble PL decay in O_2 was fitted with a biexponential function, revealing a substantial fast-decaying component with a characteristic time of ~10 s and a slower component of ~93 s, together with a relatively non-decaying background. However, the corresponding time constants were approximately 11.6 and 313.4 s under N_2, whereas the slow component becomes roughly three times longer. These results demonstrate that removal of oxygen suppresses the rapid bleaching channel and stabilizes long-lived emissive states, while oxygen-containing atmospheres promote both a higher fraction of rapidly quenched centers and a much lower residual PL intensity.

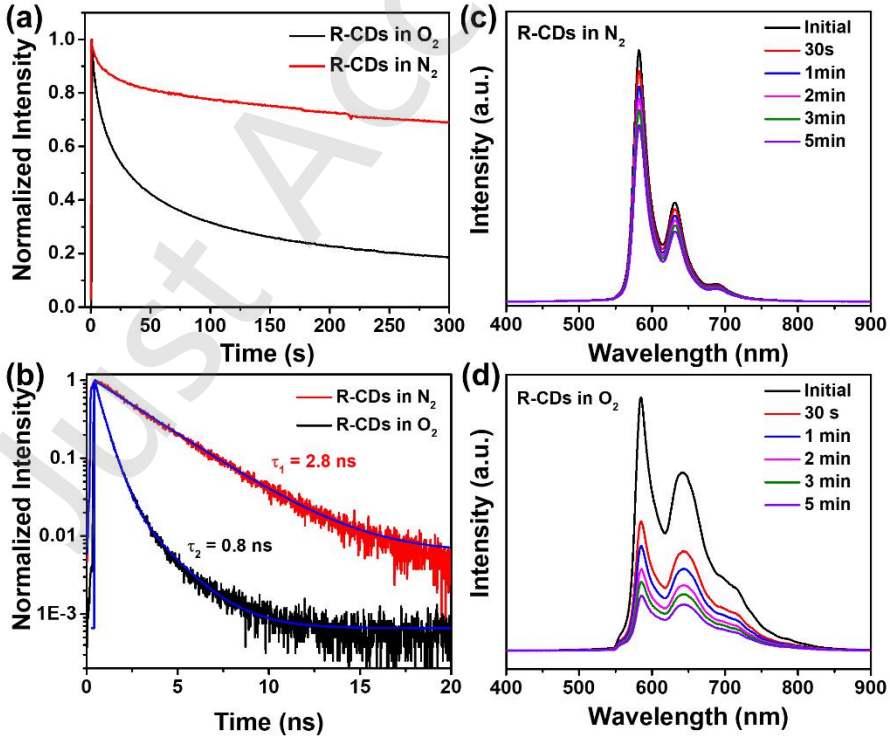


Figure 1. Atmosphere-dependent PL behavior of R-CDs. (a) Normalized ensemble PL intensity trace of the ensemble R-CDs film under N_2 and O_2 atmospheres. (b) Comparison of time-resolved PL decay curves of R-CDs under N_2 and O_2 atmospheres; (c, d) Time evolution of PL spectrum of R-CDs under N_2 atmosphere (c) andO_2 atmosphere (d).

Although PL decay reveals the oxygen-dependent photostability variation, time-resolved PL measurements were further performed to elucidate the underlying excited-state relaxation dynamics under N_2 and O_2 atmospheres (Fig. 1b). Compared with N_2, the effective PL lifetime decreased markedly from 2.8 ns to 0.8 ns under O_2 exposure, indicating the introduction of additional non-radiative relaxation pathways. The biexponential fitting results further showed that both lifetime components decreased under O_2 exposure, indicating that oxygen introduces additional non-radiative relaxation

Just Accepted

pathways associated with the heterogeneous surface environments of R-CDs. In addition to lifetime shortening, the spectral characteristics of R-CDs also exhibit notable changes in the presence of oxygen. Under N_2 , both the emission band shape and the peak maximum remain essentially unchanged during several minutes of continuous excitation (Fig. 1c). Oxygen exposure induces pronounced spectral broadening without a substantial shift of the PL peak maximum (Fig. 1d). To clarify whether the oxygen-induced spectral and lifetime changes arise from reversible modulation or irreversible modification of R-CDs, atmosphere-switching measurements following an N_2–O_2–N_2 sequence were performed. Interestingly, the PL spectrum and life partially recovered after restoring the N_2 atmosphere (Fig. S2). These reversible changes suggest that oxygen does not primarily generate new emissive species but dynamically regulates the heterogeneous emissive states of R-CDs through oxygen-mediated quenching interactions. This behavior suggests that oxygen does not simply induce a rigid shift of the emission energy, but rather causes differential quenching of surface-associated emission pathways through reversible oxygen-mediated charge transfer and trapping processes. The unequal sensitivity of these emissive contributions to oxygen results in a redistribution of the emission profile, leading to the observed spectral broadening[24-28]. More details are provided in the Supporting Information.

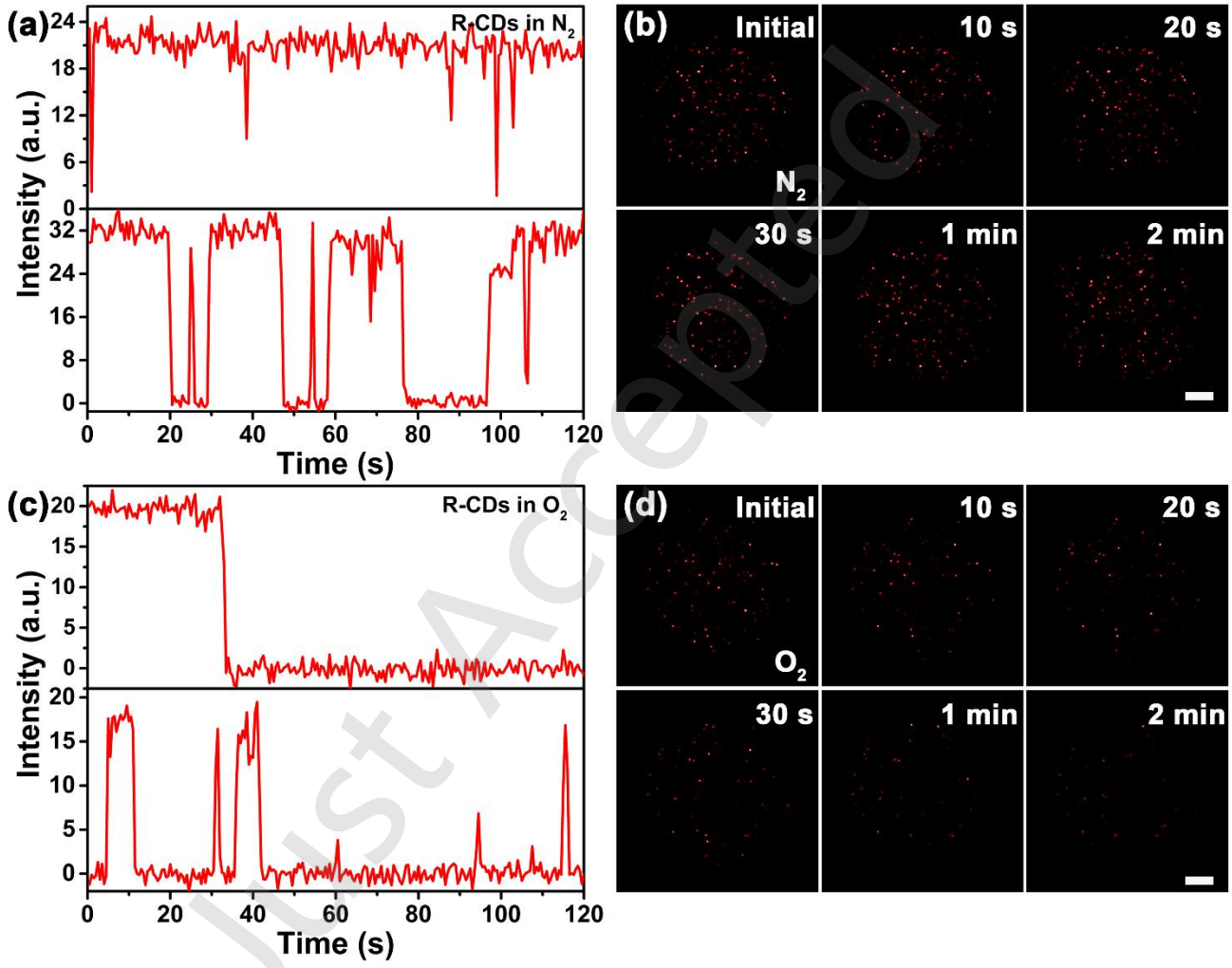


Figure 2. Single-particle PL blinking of R-CDs under N_2 and O_2 atmospheres. Representative single-particle intensity traces of the R-CDs under N_2 (a) and under O_2 atmospheres (c). (b, d) PL image sequences of R-CDs under N_2 (b) and under O_2 (d) atmospheres at the single-particle level. Scale bar, 2 μm. A 532 nm laser was used as the excitation source with a power density of 48 $W \cdot cm^{-2,}$ and the exposure time was 0.5 s.

To disentangle the atmospheric effects observed at the ensemble level and directly access single-particle kinetics, we diluted the R- CDs dispersion to the single- particle level and recorded PL trajectories under nitrogen and oxygen. Representative PL time traces acquired are shown in Fig. 2a, c, with wide- field images of the same region at different time points in Fig. 2b, d. The particles are well isolated in the field of view, however, under oxygen their spot intensities become conspicuously heterogeneous, reflecting pronounced blinking, whereas in nitrogen the spot intensities remain comparatively uniform. All CDs showed clear PL blinking with broad distributions of on/off duration ranging from seconds to hundred seconds, and most of the single CDs exhibited single on-state intensity levels. Here, we distinguish reversible dark-state from irreversible photobleaching. Dark states refer to temporary off periods followed by fluorescence recovery, whereas photobleaching corresponds to permanent fluorescence loss without recovery within the observation window. In nitrogen the CDs remain bright for extended intervals or continue to blink while sustaining emission during continuous irradiation (Fig. 2a). By contrast, in oxygen, many trajectories exhibit one- step quenching and long off-sate with only occasional returns to the

Just Accepted

on-state, with dark periods extending to tens of seconds (Fig. 2c). Quantitatively, oxygen accelerates photobleaching at the single- particle level, within 2 min more than ~70% of particles were quenched or bleached, whereas under nitrogen ~90% remain emissive over the same interval. These single- particle observations are fully consistent with the ensemble PL decay and establish that the macroscopic PL intensity loss reflects the population- averaged bleaching/quenching of individual emitters.

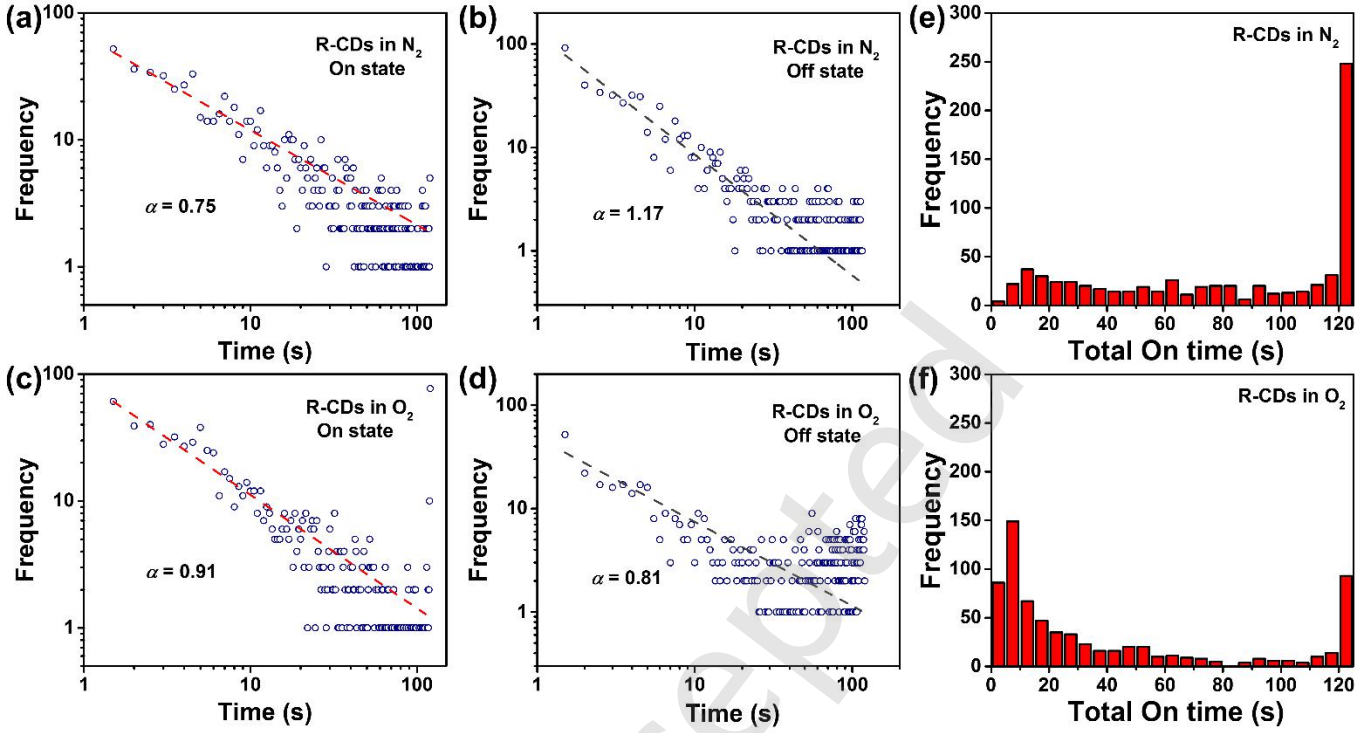


Figure 3. On- and off-state statistics of individual R-CDs under N_2 and O_2 atmospheres. (a, b) Distribution of the on-time and off-time duration of individual R-CDs (blue circles) under N_2; (c, d) corresponding distributions under O_2. The dashed line is a power law fit to the experimental data. (e, f) Distributions of total on-state durations within the total acquisition time of R-CDs under N_2 (e) and O_2, respectively. A total of ~700 individual R-CD particles were included in the statistical analysis.

To quantitatively compare the effect of atmosphere on the blinking behavior of R-CDs, we analyzed the on/off-state duration and frequency as shown in Fig. 3. The durations of both the on/off states were distributed over a wide time range, from a few hundred milliseconds to minutes. The statistics of the on/off state can be well fitted by a power law[29,30],

$$P(t_{on/off}) = At^{-\alpha}$$

where P(t) is the probability of blinking events and α is the exponential coefficient of the power law, which represents the probability of observing blinking events with a given duration and α is the scaling exponent characterizing the statistical distribution of on/off-state durations. A smaller α indicates a slower decay of the distribution, corresponding to a higher probability of long-lived on/off events. The on-state exponent increased from 0.75 to 0.91, whereas the off-state exponent decreased from 1.17 to 0.81 upon changing from N_2 to O_2.

To further quantify the oxygen-induced modulation of intermittency in the time domain, we integrated total on and off time within each trajectory to obtain the cumulative on- and off-state occupancies. Under N_2 , individual R-CDs spend on average 77.9 s in the on state, whereas this value decreases to 27.7 s in O_2 (Fig. 3 e, f), evidencing a pronounced reduction of the effective emissive duty cycle upon oxygen exposure. Consistently, the mean on-state duration shortens from 45.6 s (N_2) to 28.9 s (O_2), while the mean off-state duration increases from 24.1 s to 52.1 s, indicating that oxygen not only enhances on-state termination but also stabilizes long-lived non-emissive configurations. In line with this trend, the fraction of particles remaining bright for >90% of the observation window drops from 43% in N_2 to 17% in O_2 , underscoring the strong propensity of oxygen to bias the blinking dynamics toward extended off state occupancy under continuous excitation. It is worth noting that increasing the excitation power density similarly accelerates the photobleaching rate of the R-CDs, which is consistent with photoinduced charge separation and trap-filling mechanisms previously established for CDs. To isolate genuine environmental modulations from power-dependent artifacts, all optical measurements in this study were conducted under a well-controlled, moderate excitation power.

This change could be rationalized within a trap-/charging-mediated intermittency framework that is widely used for SQDs, where stochastic photoionization and subsequent nonradiative loss in the charged configuration produce intensity intermittency with power-law on/off distributions[30,31]. In our case, introducing O_2 increases the probability that an emitter leaves the neutral state during illumination, as evidenced macroscopically by the pronounced lifetime shortening and the emergence of bi-exponential decay in the film, which is a signature of added nonradiative deactivation channels and heterogeneous quenching efficiencies[32]. At the single-particle level, this additional nonradiative pathway is naturally assigned to dynamic quenching of the emissive excited state, which increases the on-state termination and therefore suppresses long on-state events, consistent with the observed increase in the on-state power-law exponent. Crucially, oxygen as a strong external electron acceptor under photoexcitation, can also bias the CDs

Just Accepted

toward long-lived non-emissive state by stabilizing charge-separated/trapped states (e.g., via photoinduced electron transfer and subsequent slow neutralization), which increases the statistical weight of long off-state events and accounts for the decreased off-state exponent.

Considering the formation process of CDs, a shell layer resembling conjugated polymers may exist on or be connected to the surface of CDs, which can also induce PL blinking through energy transfer or conformational changes [17,29]. Meanwhile, low temperatures often suppress interference caused by the thermal motion of fluorescent materials themselves, allowing for a closer approximation to the intrinsic properties. Therefore, to further elucidate the intrinsic mechanism of CDs blinking, we performed a systematic analysis of the blinking behavior of R-CDs at low temperatures. Figure 4 shows typical PL intensity traces of R-CDs at different temperatures, with statistical results presented in Fig. S3-S5. Statistical results indicate that as the temperature decreases, CDs become more stable under sustained excitation, the off-state duration shortens, and prolonged off states occur less frequently. Importantly, the α values for the on-state fluctuated around 1 at various temperatures, while the α values for the off-state fluctuated around 1.4 without a systematic temperature dependence. Such near temperature-invariant power-law blinking is a hallmark of scale-free intermittency in single emitters and has been widely documented for SQDs, where it is commonly interpreted in terms of broadly distributed trapping/de-trapping barriers and tunneling- or diffusion-controlled charge transfer dynamics rather than a single thermally activated rate-limiting step [33-35].

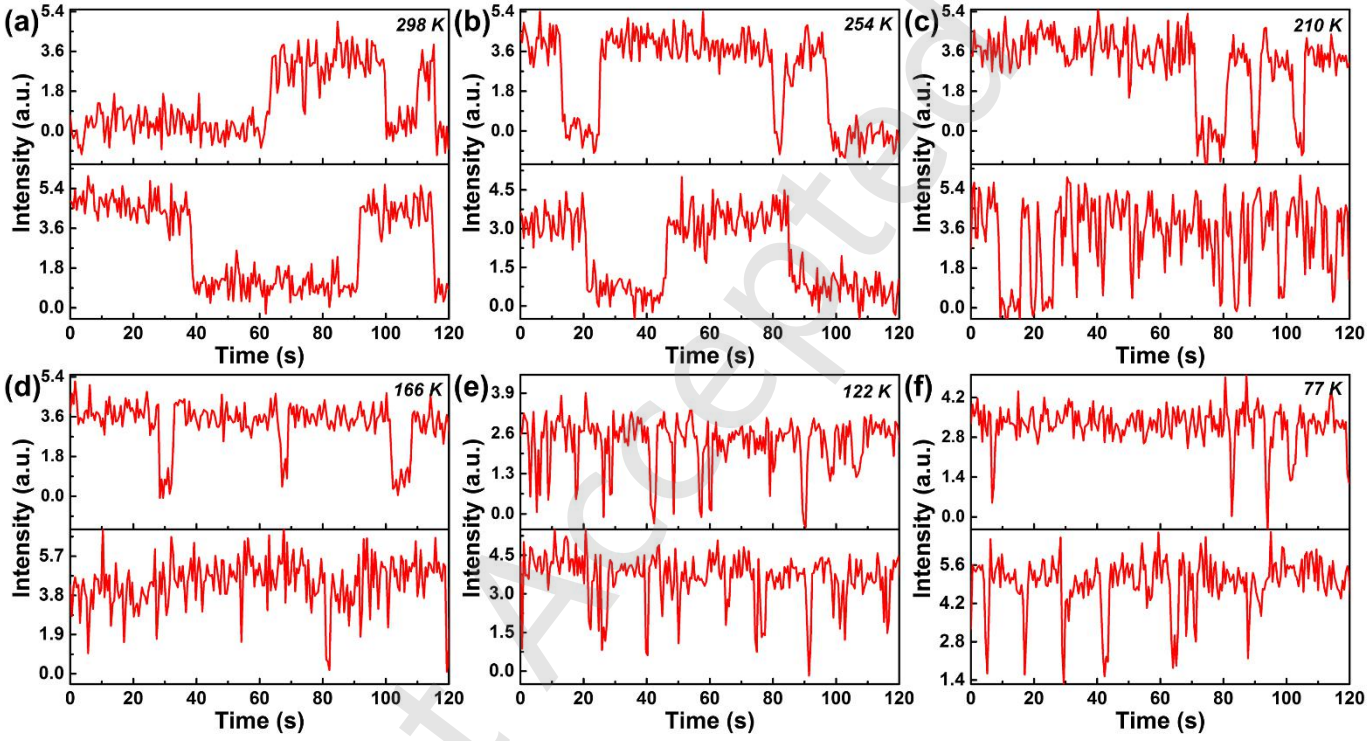


Figure 4. Representative PL intensity trajectories of individual R-CDs at different temperatures from 77 to 298 K: (a) 298 K; (b) 254 K; (c) 210 K; (d)166 K; (e) 122 K; and (f) 77 K. Approximately 300 individual R-CD particles were investigated at each temperature.

To further quantify the temperature-dependent modulation of blinking dynamics, the duty cycle and switching rates were analyzed. The duty cycle (DC), defined as the fraction of the acquisition time spent in the emissive ("on") state, DC=T_{on} / (T_{on} + T_{off}), which provides a robust metric for comparing photostability across temperatures under a fixed on/off definition. The DC was markedly higher at low temperatures, reaching 0.719 at 77 K and 0.721 at 122 K, corresponding to a total on time of approximately 86 s, whereas it decreased to approximately 0.53 at higher temperatures (Fig. S6 and S7). Interestingly, the fitted power-law exponents of the on/off-duration distributions remained nearly unchanged over the investigated temperature range despite the pronounced variation in DC. These observations are not contradictory because the two parameters describe different aspects of fluorescence intermittency. The power-law exponent characterizes the scaling behavior of the on/off-duration distributions, whereas the DC is an integrated measure determined by the relative cumulative residence times in the on and off states. Thus, the power-law exponent alone does not determine the DC, and changes in transition kinetics can alter on/off occupancy without necessarily producing a pronounced change in the fitted power-law exponent.

To identify the kinetic origin of the temperature-dependent DC, we further performed a model-free analysis using effective switching rates. Only reversible blinking events identified by thresholded binary traces were counted (with on–off–on or off–on–off counted as one blinking; irreversible quenching/photobleaching excluded), so that each blinking corresponds to one on→off and one off→on transition. We then defined $k_{on\rightarrow off} = N_{blinking} / T_{on}$ and $k_{off\rightarrow on} = N_{blinking} / T_{off}$, which quantify the propensity to leave the on state and to recover from the off state, respectively. These parameters are treated as effective switching rates derived from the statistical analysis of blinking trajectories, describing the average switching behavior between emissive and non-emissive states rather than intrinsic microscopic rate constants of a specific molecular transition. The temperature dependence of the blinking-event frequency is

Just Accepted

shown in Fig. S7. Although trajectories with relatively few switching events remain predominant, the contribution from trajectories exhibiting multiple reversible switching events becomes more pronounced at low temperatures. More importantly, the dominant systematic change is an acceleration of off state recovery: the median $k_{off\rightarrow on}$ increases from 0.0159 s^{-1} at 298 K to 0.0796 s^{-1} at 77 K and 0.122 s^{-1} at 122 K, whereas the median $k_{on\rightarrow off}$ stays within the same $\sim 10^{-2}$ s^{-1} range without a comparable reorganization. Taken together, the higher duty cycle at low temperature is therefore primarily attributable to enhanced off-state reversibility, that is, reduced effective occupation of deep or long-lived off states, rather than to strong suppression of on-state termination.

To rationalize the temperature‐dependent blinking behavior of R-CDs, we consider the relaxation and recombination pathways following photoexcitation and discuss how transitions between emissive ("on") and quenched ("off") states can be modulated by temperature. Upon optical excitation, electron-hole pairs are generated and relax to emissive states on sub-picosecond-to-picosecond timescales through phonon-mediated energy dissipation[36,37]. Importantly, the emissive states in CDs do not typically correspond to a single discrete level, but rather to an ensemble of states arising from multiple emissive centers, including the carbon core or localized sp^2-conjugated domains, surface states associated with functional groups, and, in some cases, molecular or crosslink-related emissive centers[3,17]. Once these emissive states are populated, radiative recombination gives rise to fluorescence corresponding to the "on" state in single-particle trajectories. Alternatively, excitation can be diverted into nonradiative pathways, leading to "off" or intermediate "grey" states. Two broad quenching pathways are commonly discussed: (i). defect-mediated nonradiative recombination, in which carriers are captured by surface or interfacial defects, functional-group-related states, or environmental acceptors, followed by energy dissipation through multiphonon relaxation; (ii) photoinduced charging or charge separation, which suppresses radiative recombination through efficient nonradiative pathways and/or enhanced quenching arising from interactions between excess charges and local electronic states. Because CDs are structurally and chemically heterogeneous, key parameters such as trap depth, spatial location,

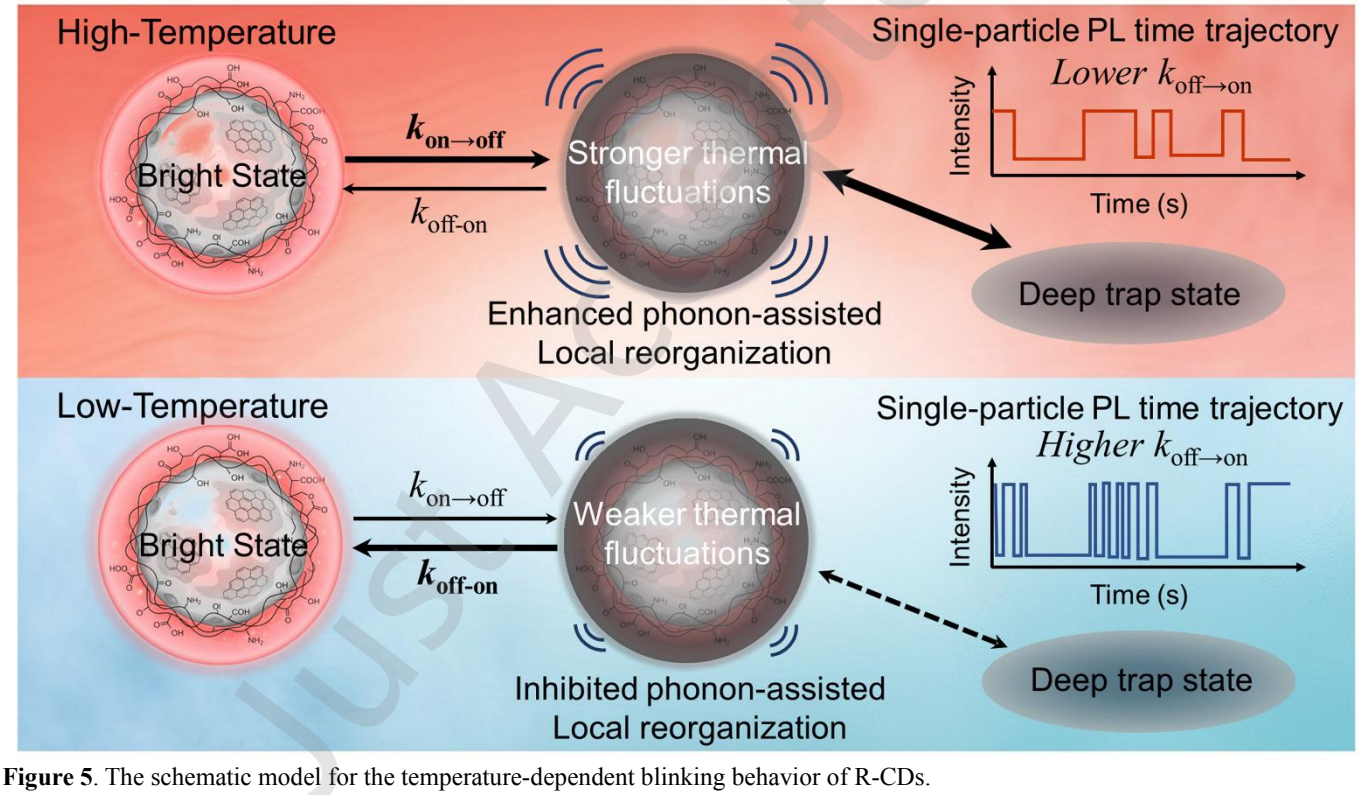


Figure 5. The schematic model for the temperature-dependent blinking behavior of R-CDs.

coupling strength to emissive centers, and the local dielectric environment can vary substantially across different local sites. Consequently, switching between on and off states is not expected to be governed by a single, well-defined activation barrier. Instead, it can be viewed as stochastic carrier transfer among a distribution of local states, proceeding via phonon-assisted hopping between traps and, in some cases, via tunneling-mediated transfer and recovery. Within such a distributed-state, the power-law exponent can remain relatively insensitive to temperature over a certain range, whereas temperature primarily modulates the statistical weight of long-lived off states rather than the underlying origin of the power-law form.

In this context, the distinct temperature dependences of the two effective switching rates ($k_{on\rightarrow off}$ and $k_{off\rightarrow on}$), together with the shortening of off-state duration or prolonged off-state events at low temperatures, suggest that the off-state is not a single kinetic state but comprises multiple branches with different degrees of stability, which can be phenomenologically described as relatively shallow and deep off-states. Once carrier is trapped, the system may continue to undergo local reorganization that lowers the trap energy and further localizes the carrier, for example through conformational changes of surface functional groups or local atomic rearrangements (Fig. 5). These processes rely on coupling to thermal phonon fluctuations, which facilitate configurational exploration and energy dissipation, and can further stabilize the trapped charge, thereby deepening the trap and promoting the formation of longer-lived deep off states. As

Just Accepted

the temperature decreases, the reduced thermal phonon population and the increased difficulty of crossing small configurational barriers hinder such rearrangements, lowering the probability of accessing the deep-off-state branch and thereby suppressing long off events. Consistent with this interpretation, the effective $k_{off\rightarrow on}$ from 0.0159 s^{-1} at 298 K to 0.122 s^{-1} at 122 K, whereas $k_{on\rightarrow off}$ remains within the same order of magnitude. Correspondingly, the DC increases from approximately 0.53 at higher temperatures to 0.721 at 122 K, equivalent to a decrease in the off-state occupancy from approximately 47% to 27.9%, respectively. As a result, the overall off-state occupancy decreases, leading to a higher duty cycle and an apparent increase in the effective off→on recovery rate.

Conclusions

In conclusion, this work shows that the PL instability of CDs under continuous excitation is governed by heterogeneous single-particle CDs dynamics rather than by a uniform bleaching process. By resolving the effects of atmosphere and temperature at the single-particle level, we find that oxygen favors the formation of long-lived off states and accelerates irreversible photobleaching, whereas cooling increases the effective occupation of emissive states by improving dark-state reversibility. These findings indicate that the photostability of CDs is determined not only by the rate of permanent photochemical degradation, but also by the kinetics with which emitters enter, remain in, and recover from non-emissive states. More broadly, this work provides a mechanistic framework for understanding the interplay between blinking and photobleaching in structurally heterogeneous CDs. Such insight should facilitate more rigorous evaluation of fluorescence stability and guide the design of carbon dots with improved operational reliability in long-term imaging, sensing, and related applications.

Electronic Supplementary Material: Supplementary material (Experimental Procedures, PL decay fitting curves, Atmosphere-dependent PL spectra and fluorescence decay dynamics, Statistical Analysis of single-particle cds blinking behavior) is available in the online version of this article at https://doi.org/10.26599/NR.2026.94909226.

Data availability

All data needed to support the conclusions in the paper are presented in the manuscript and/or the Electronic Supplementary Material. Additional data related to this paper may be requested from the corresponding author upon request.

Acknowledgements

This work is granted by the National Natural Science Foundation of China (No. 22505234), Natural Science Foundation of Henan (No. 252300421728), the Fundamental Research Funds for the Central Universities (No. 2025TJJBKY002, 2025TJJBKY001, 2025TJJBKY005, 2025TJJBKY007), Henan Provincial Key Scientific Research Projects for Higher Education Institutions (No. 26B150028, 26B430034), and the College Students' Innovation and Entrepreneurship Training Program (No. 20261273530). The authors would like to thank Zhengzhou University of Science and Technology for providing the necessary support for this research.

Declaration of competing interest

All the contributing author(s) report(s) no conflict of interests in this work.

Author contribution statement

Z. W.: Funding acquisition, supervision, experimental design, writing – review & editing. Y. O.: Data curation, project administration, validation, experimental design. J. C., J. H, D. L.: Funding acquisition, Experiment implementation, formal analysis. Y. L., S.L., and B. W.: Data curation, formal analysis. W. L., S. L. and Y. T.: Project administration, Funding acquisition, verified the data accuracy. All the authors have approved the final manuscript.

Use of AI statement

None.

References

[1] Yang, Z.; Xu, T.; Li, H.; She, M.; Chen, J.; Wang, Z.; Zhang, S.; Li, J. Zero-Dimensional Carbon Nanomaterials for Fluorescent Sensing and Imaging. *Chem. Rev*. **2023**, *123*, 11047–11136.

[2] Wang, B.; Lu, S. The Light of Carbon Dots: From Mechanism to Applications. *Matter* **2022**, *5*, 110–149.

[3] Đorđević, L.; Arcudi, F.; Cacioppo, M.; Prato, M. A Multifunctional Chemical Toolbox to Engineer Carbon Dots for Biomedical and Energy Applications. *Nat. Nanotechnol*. **2022**, *17*, 112–130.

[4] Zhu, P.; Wang, S.; Zhang, Y.; Li, Y.; Liu, Y.; Li, W.; Wang, Y.; Yan, X.; Luo, D. Carbon Dots in Biomedicine: A Review. *ACS Appl. Bio Mater*. **2022**, *5*, 2031–2045.

[5] Mkhari, O.; Ntuli, T. D.; Coville, N. J.; Nxumalo, E. N.; Maubane-Nkadimeng, M. S. Supported Carbon-Dots: A Review. *J. Lumin.* **2023**, *255*, 119552.

[6] Dua, S.; Kumar, P.; Pani, B.; Kaur, A.; Khanna, M.; Bhatt, G. Stability of Carbon Quantum Dots: A Critical Review. *RSC Adv*. **2023**, *13*, 13845–13861.

[7] Ha, T.; Fei, J.; Schmid, S.; Lee, N. K.; Gonzalez, R. L.; Paul, S.; Yeou, S. Fluorescence Resonance Energy Transfer at the Single-Molecule Level. *Nat Rev Method. Prime.* **2024**, *4*, 21.

[8] Nettels, D.; Galvanetto, N.; Ivanović, M. T.; Nüesch, M.; Yang, T.; Schuler, B. Single-Molecule FRET for Probing Nanoscale Biomolecular Dynamics. *Nat. Rev. Phys.* **2024**, *6*, 587–605.

[9] Qin, H.; Meng, R.; Wang, N.; Peng, X. Photoluminescence Intermittency and Photo‐Bleaching of Single Colloidal Quantum Dot. *Adv. Mater.* **2017**, *29*, 1606923.

[10] Yang, L.; Zheng, Y.; Ye, Z.; Xiao, Y. Single-Molecule Fluorescence Defines a New Dye Chemistry. *Chem. Biomed. Imaging* **2026**, *4*, 510–526.

[11] Zhang, L.; Shen, D.; Yang, J. Advancing Single-Molecule Biophysics: Next-Generation Organic Fluorophores with Tailored Labeling Strategies. *Chem. Biomed. Imaging* **2025**, *3*, 572–598.

[12] Stennett, E. M. S.; Ciuba, M. A.; Levitus, M. Photophysical Processes in Single Molecule Organic Fluorescent Probes. *Chem. Soc. Rev*. **2014**, *43*, 1057–1075.

[13] Efros, A. L.; Nesbitt, D. J. Origin and Control of Blinking in Quantum Dots. *Nat. Nanotechnol*. **2016**, *11*, 661–671.

[14] Li, B.; Zhang, G.; Gao, Y.; Chen, X.; Chen, R.; Qin, C.; Hu, J.; Wu, R.; Xiao, L.; Jia, S. Single Quantum Dot Spectroscopy for Exciton Dynamics. *Nano Res*. **2024**, *17*, 10332–10345.

[15] Feld, L. G.; Shynkarenko, Y.; Krieg, F.; Rainò, G.; Kovalenko, M. V. Perovskite Quantum Dots for Super‐Resolution Optical Microscopy: Where Strong Photoluminescence Blinking Matters. *Adv. Opt. Mater.* **2021**, *9*, 2100620.

[16] Zhi, S.; Dai, Q.; Wang, H.; Wu, D.; Zhao, L.; Hu, C.; Dai, L. Heteroatom-Doped Carbon Materials for Multifunctional Noncatalytic Applications. *ACS Nano* **2025**, *19*, 29860–29897.

Just Accepted

[17] Wang, B.; Waterhouse, G. I. N.; Yang, B.; Lu, S. Advances in Shell and Core Engineering of Carbonized Polymer Dots for Enhanced Applications. *Acc. Chem. Res*. **2024**, *57*, 2928–2939.

[18] Fu, Q.; Ma, Z.; Sun, S.; Zhang, K.; Zhan, Y.; Liu, D. Elementally Doped Carbonized Polymer Dots: Control of Optical Properties and Their Versatile Applications. *Adv. Opt. Mater*. **2025**, *13*, 2403251.

[19] Cai, L.; Liu, J.; Liu, J.; Guo, Z.; He, Y.; Pan, Y.; Ran, X.; Liu, R.; Guo, L.; Qu, S. Chiral Transcription on Achiral Carbon Dots by Linking with Chiral Histidine for pH‐Tunable Dual‐Mode Chiroptical Switch in Circular Dichroism and Circularly Polarized Luminescence. *Angew Chem. Int. Ed.* **2026**, *65*, e4871915.

[20] Zhang, Q.; Wang, R.; Feng, B.; Zhong, X.; Ostrikov, K. Photoluminescence Mechanism of Carbon Dots: Triggering High-Color-Purity Red Fluorescence Emission through Edge Amino Protonation. *Nat. Comm.* **2021**, *12*, 6856.

[21] Tan, J.; Lu, C.; Gu, X.; Jiang, Z.; Gu, H.; Jin, Z.; Qu, S.; Li, Q.; Ding, J. Wide‐Gamut and Reversible Phosphorescence Tuning From Green to NIR in Carbon Dots via Acid‐Responsive Protonation‐Assembly Strategy. *Adv. Funct. Mater*. **2026**, *36*, e23830.

[22] Guo, Z.; Bian, Y.; Zhang, L.; Zhang, J.; Sun, C.; Cui, D.; Lv, W.; Zheng, C.; Huang, W.; Chen, R. Multi‐Stimuli‐Responsive Carbon Dots with Intrinsic Photochromism and In Situ Radical Afterglow. *Adv. Mater*. **2024**, *36*, 2409361.

[23] Liu, X.; Feng, N.; Sun, X.; Li, H. Polarity Adaptive Carbon Dots: Photoluminescence in Heterogeneous Environments. *Adv. Opt. Mater*. **2025**, *13*, 2403394.

[24] Wang, C.; Fang, Y.; Zhou, D.; Wu, C.; Zhu, H.; Song, Q. Surface Oxidation of Carbon Dots Enables Highly Selective and Sensitive Chemiluminescence Detection of Hydroxyl Radical. *Nano Res*. **2024**, *17*, 9275–9283.

[25] Wang, L.; Zhang, X.; Yang, K.; Wang, L.; Lee, C.-S. Oxygen/Nitrogen-Related Surface States Controlled Carbon Nanodots with Tunable Full-Color Luminescence: Mechanism and Bio-Imaging. *Carbon* **2020**, *160*, 298–306.

[26] Nayana, K.; Sunitha, A. P. Temperature Dependent Downconversion Photoluminescence of Naturally Synthesized Carbon Dots. *J Opt.* **2025**:1-7.

[27] Ghosh, S.; Chizhik, A. M.; Karedla, N.; Dekaliuk, M. O.; Gregor, I.; Schuhmann, H.; Seibt, M.; Bodensiek, K.; Schaap, I. A. T.; Schulz, O.; Demchenko, A. P.; Enderlein, J.; Chizhik, A. I. Photoluminescence of Carbon Nanodots: Dipole Emission Centers and Electron–Phonon Coupling. *Nano Lett*. **2014**, *14*, 5656–5661.

[28] Wang, B.; Wei, Z.; Sui, L.; Yu, J.; Zhang, B.; Wang, X.; Feng, S.; Song, H.; Yong, X.; Tian, Y.; Yang, B.; Lu, S. Electron–Phonon Coupling-Assisted Universal Red Luminescence of o-Phenylenediamine-Based Carbon Dots. *Light Sci. Appl.* **2022**, *11*, 172.

[29] Wei, Z.; Yang, X.; Liao, C.; Shan, F.; Feng, S.; Ye, S.; Hou, X.; Wang, L.; Wang, X.; Wang, Z.; Lu, S.; Tian, Y. Heteroatom Doping Effects on the Exciton Behavior in Carbonized Polymer Dots. *Nano Lett*. **2025**, *25*, 4013–4021.

[30] Khan, S.; Li, W.; Karedla, N.; Thiart, J.; Gregor, I.; Chizhik, A. M.; Enderlein, J.; Nandi, C. K.; Chizhik, A. I. Charge-Driven Fluorescence Blinking in Carbon Nanodots. *J. Phys. Chem. Lett*. **2017**, *8*, 5751–5757.

[31] Wei, Z.; Wang, B.; Hong, D.; Xie, M.; Wan, S.; Yang, W.; Lu, S.; Tian, Y. Rational Building of Nonblinking Carbon Dots via Charged State Recovery. *J. Phys. Chem. Lett*. **2021**, *12*, 8614–8620.

[32] Zu, F.; Yan, F.; Bai, Z.; Xu, J.; Wang, Y.; Huang, Y.; Zhou, X. The Quenching of the Fluorescence of Carbon Dots: A Review on Mechanisms and Applications. *Microchim. Acta* **2017**, *184*, 1899–1914.

[33] Gerhard, M.; Louis, B.; Camacho, R.; Merdasa, A.; Li, J.; Kiligaridis, A.; Dobrovolsky, A.; Hofkens, J.; Scheblykin, I. G. Microscopic Insight into Non-Radiative Decay in Perovskite Semiconductors from Temperature-Dependent Luminescence Blinking. *Nat. Comm.* **2019**, *10*, 1698.

[34] Chon, B.; Bang, J.; Park, J.; Jeong, C.; Choi, J. H.; Lee, J.-B.; Joo, T.; Kim, S. Unique Temperature Dependence and Blinking Behavior of CdTe/CdSe (Core/Shell) Type-II Quantum Dots. *J. Phys. Chem. C* **2011**, *115*, 436–442.

[35] Shimizu, K. T.; Neuhauser, R. G.; Leatherdale, C. A.; Empedocles, S. A.; Woo, W. K.; Bawendi, M. G. Blinking Statistics in Single Semiconductor Nanocrystal Quantum Dots. *Phys. Rev. B* **2001**, *63*, 205316.

[36] Nguyen, H. A.; Srivastava, I.; Pan, D.; Gruebele, M. Unraveling the Fluorescence Mechanism of Carbon Dots with Sub -Single-Particle Resolution. *ACS Nano* **2020**, *14*, 6127–6137.

[37] Nguyen, H. A.; Srivastava, I.; Pan, D.; Gruebele, M. Ultrafast Nanometric Imaging of Energy Flow within and between Single Carbon Dots. *Proc. Natl. Acad. Sci. U.S.A*. **2021**, *118*, e2023083118.

© The Author(s) 2026. *Nano Research* published by Tsinghua University Press. The articles published in this open access journal are distributed under the terms of the Creative Commons Attribution 4.0 International License (http://creativecommons.org/licenses/by/4.0/), which permits use, distribution and reproduction in any medium, provided the original work is properly cite

Just Accepted

Electronic Supplementary Material

Atmosphere and temperature regulated fluorescence intermittency of carbon dots from single-particle dynamics to ensemble photostability

Zhihong Wei[1,2,§], Yixin Ouyang[2,§], Juan Chen[1], Jingtao Huang[1], Denghui Liu[1], Yiru Jiang[1], Sen Luo[2], Boyang Wang[3], Wei, Li[1], Siyu Lu[3,✉], and Yuxi Tian[2,✉]

[1] *Department of Forensic Science and Technology, Zhengzhou Police University, Zhengzhou 450000, China*
[2] *State Key Laboratory of Analytical Chemistry for Life Science, Key Laboratory of Mesoscopic Chemistry of MOE, School of Chemistry, Nanjing University, Nanjing 210023, China*
[3] *Green Catalysis Center, and College of Chemistry, Zhengzhou University, Zhengzhou 450000, China*

Supporting information to https://doi.org/10.26599/NR.2026.94909226

Just Accepted

Experimental Procedures

Chemicals and materials.

O-phenylenediamine (oPD), H_2SO_4, were purchased from Sigma-Aldrich Co. LLC. All chemicals were employed directly without additional purification. Redistilled water used in the experiments was prepared with an SZ-93A water purification system. All reagents were analytical grade and used as received.

Preparation of the Carbonized polymer dots (CDs).

oPD (108 mg), 10 mL of redistilled water, and 100 μL H_2SO_4 were added to a 25 mL autoclave and heated at 200°C for 6 h. After cooling to room temperature, the solution was centrifuged at 10000 rpm for 5 min, then filtrated through a 0.22 μm filter membrane, and finally dialyzed with the membrane (1000 Da) for 7 days to remove the unreacted precursor and acid. The liquid in the dialysis bag is centrifuged; the precipitate is washed several times and then freeze-dried.

Glass Substrate

High-quality coverslips from Corning, Inc. were used as the substrate. The coverslips were cleaned in water and ethanol with ultrasonic treatment for 40 min each. The coverslips were then rinsed in ultrapure water, dried with nitrogen, and exposed to ultraviolet radiation for 1 h before use.

Preparation of single-particle CDs samples

The samples were prepared by the ultrasonic dissolution of a suitable amount of R-CDs in water (1 mg/mL) and then diluting the solution to a concentration of 1×10^{-6} –1×10^{-7} mg/mL. Then, the diluted CDs solutions were spin-coated on glass slide with a precovered PVA film at 1500 rpm followed by annealing at 80°C for 2 min.

Single CDs measurements, analysis and threshold Determination

The optical measurement on individual CDs were performed on a home-built widefield microscope with 532-nm CW diode laser as the light source. The PL was collected by an oil immersion objective lens (Olympus UPlanFLN 60×, NA = 1.25) and imaged by an EMCCD camera (iXon Ultra 888, Andor), after passing through a 550-nm long-pass filter (ET550lp, Chroma). PL lifetime measurements were done using a single-photon counting system (TCSPC, Picoharp 300) with 532 nm excitation light from a supercontinuous laser (Fianium SC-400, 40 MHz).

To ensure the statistical reliability and comparability across different experimental conditions, we maintained a consistent and statistically robust sample size for each set of single-particle measurements. For the atmosphere-dependent measurements, a total of ~700 well-isolated individual R-CD particles were analyzed. For the temperature-dependent measurements, approximately 300 individual R-CD particles were investigated at each temperature. The intensity traces of individual CDs were obtained by averaging a total of 10×10 pixels for each dot and subtracting the surrounding background. For the blinking analysis of each trajectory, the

Address correspondence to Yuxi Tian, tyx@nju.edu.cn; Siyu Lu, sylu2013@zzu.edu.cn

baseline emissive (on-state) and non-emissive (off-state) average intensity levels were first determined after excluding extreme intensity outliers. The threshold for state discrimination was then set at one-third of the intensity difference between the average on- and off-state levels, ensuring robust and reliable separation of the blinking states against intensity fluctuations and background noise.

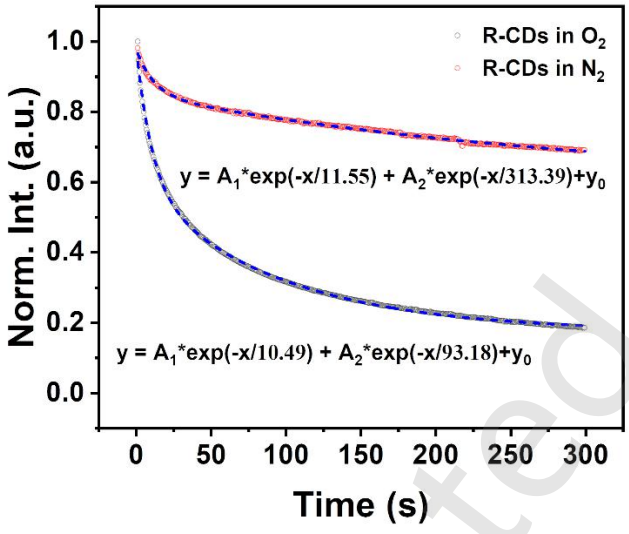


Figure S1. PL decay curves of R-CDs under O_2 and N_2 atmosphere. The fitting functions are provided in the plot (blue dashed lines) with a biexponential function.

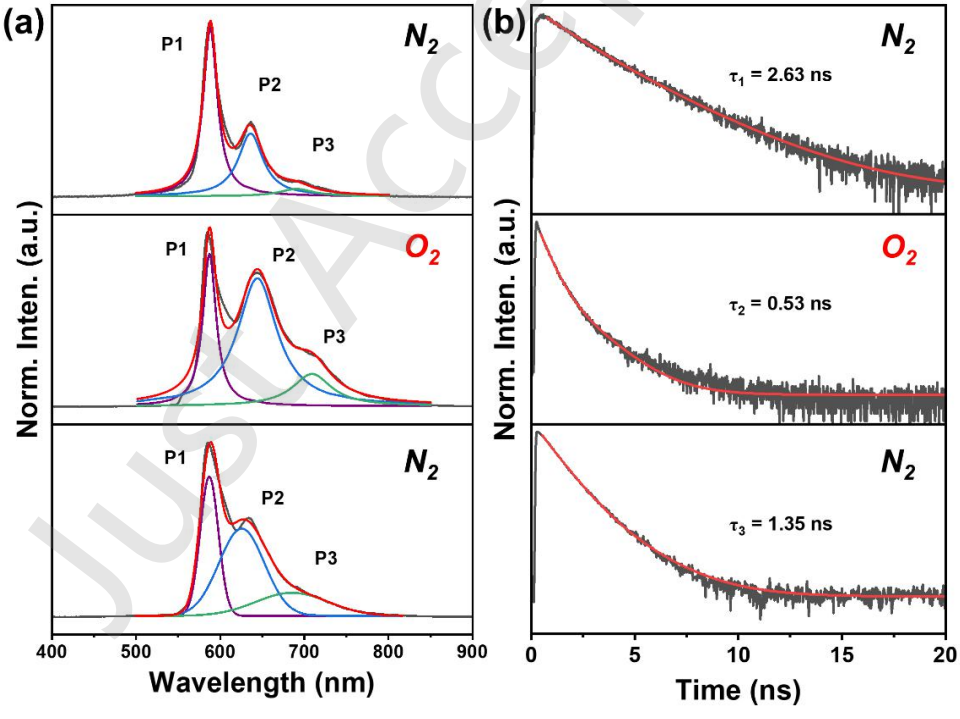


Figure S2 Atmosphere-dependent PL spectra and fluorescence decay dynamics of the R-CDs. (a) Normalized PL emission spectra of the R-CDs under the initial N_2 atmosphere (top), after exposure to O_2 (middle), and after subsequent restoration of the N_2 atmosphere (bottom). The experimental spectra are shown in gray, the overall fitted curves in red, and the three components (P1–P3) in purple, blue, and green, respectively. (b) Corresponding time-resolved fluorescence decay profiles under the initial N_2 atmosphere (top), O_2 atmosphere (middle), and restored N_2 atmosphere (bottom). The experimental decay traces are shown in gray and the fitted decay curves in red.

To clarify the origin of the pronounced spectral difference between N_2 and O_2 and to determine whether the O_2-induced broadening arises from a reversible excited-state process or an irreversible modification of the R-CDs, we performed atmosphere-switching measurements following an N_2–O_2–N_2 sequence and analyzed both the PL spectra and fluorescence decay dynamics (Fig. S2). For the PL spectra, the emission was deconvoluted into three components, P1 (~585 nm), P2 (~630 nm), and P3 (~690 nm). Under the initial N_2 atmosphere, their relative spectral contributions were 46.65%, 40.94%, and 12.41%, respectively. Upon exposure to O_2, the P1

Just Accepted

contribution decreased markedly to 25.11%, whereas P2 and P3 increased to 49.27% and 25.62%, indicating a pronounced redistribution of the spectral weight toward the long-wavelength side rather than an absolute enhancement of long-wavelength emission. After switching back to N_2, the P1, P2, and P3 contributions partially recovered to 31.49%, 47.56%, and 20.94%, respectively, accompanied by a clear narrowing of the emission profile. The substantial reversibility of the spectral distribution indicates that the O_2-induced broadening is dominated by a reversible O_2-dependent photophysical interaction rather than by the irreversible formation of a new emissive species. For the fluorescence dynamics, the effective lifetime decreased sharply from 2.63 ns under the initial N_2 atmosphere to 0.53 ns under O_2 and then partially recovered to 1.35 ns after N_2 was restored. Consistently, biexponential fitting showed that τ_1 changed from 1.890 ns (N_2) to 0.452 ns (O_2) and subsequently recovered to 0.859 ns, while τ_2 changed from 3.573 to 1.391 and then to 1.955 ns. These results demonstrate that O_2 introduces an additional excited-state nonradiative deactivation pathway, resulting in substantially accelerated fluorescence decay. The partial recovery of both the spectral profile and fluorescence lifetime after O_2 removal further supports that this process is largely reversible and governed by oxygen-mediated photophysical interactions rather than irreversible alteration of R-CDs. Importantly, the simultaneous lifetime shortening and redistribution of normalized spectral components indicate that oxygen-induced quenching is not uniform among surface-associated emission pathways. Instead, oxygen-mediated charge transfer and trapping processes differentially modulate these pathways, resulting in a redistribution of emission contributions and the observed spectral broadening rather than a simple rigid shift of the emission energy.

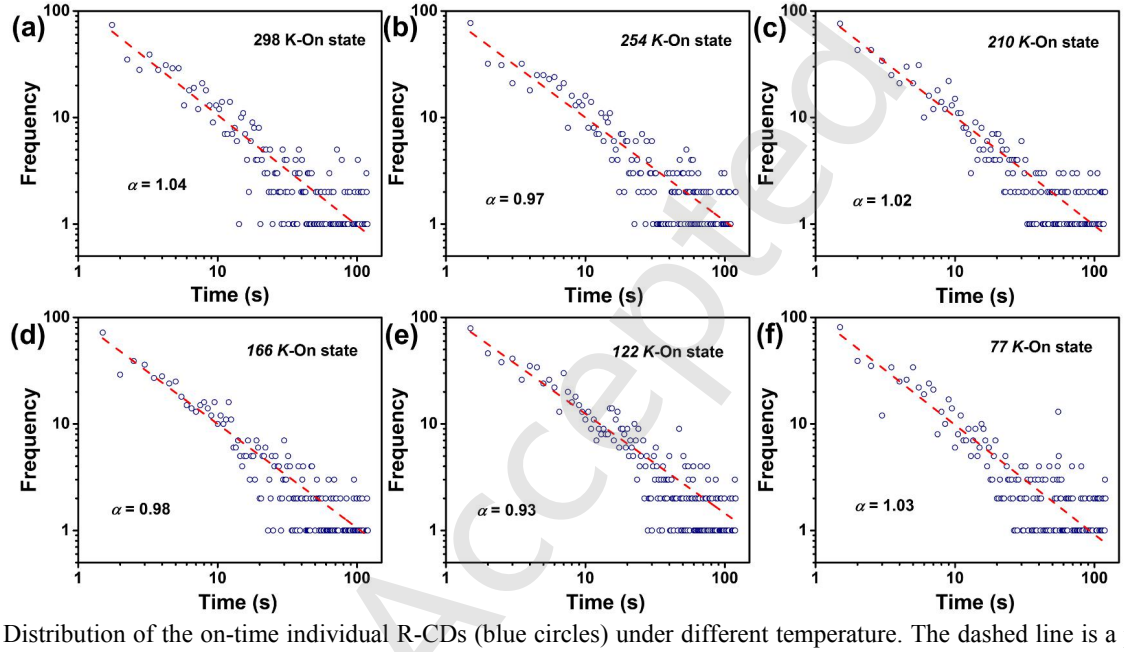


Figure S3. Distribution of the on-time individual R-CDs (blue circles) under different temperature. The dashed line is a power law fit to the experimental data.

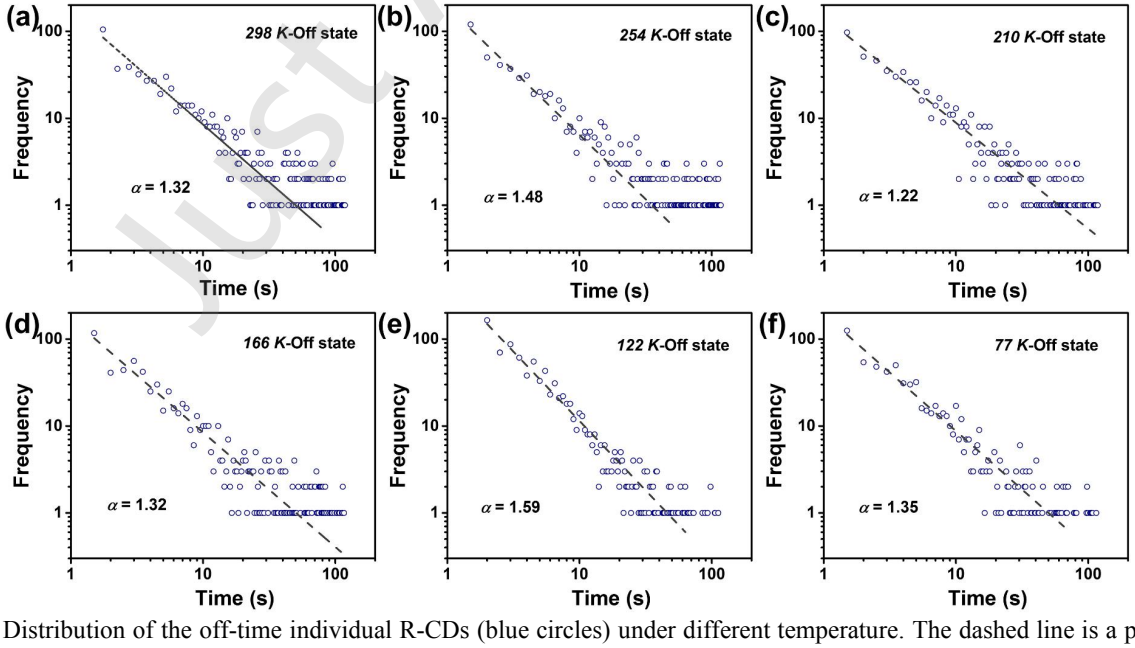


Figure S4. Distribution of the off-time individual R-CDs (blue circles) under different temperature. The dashed line is a power law fit to the experimental data.

Just Accepted

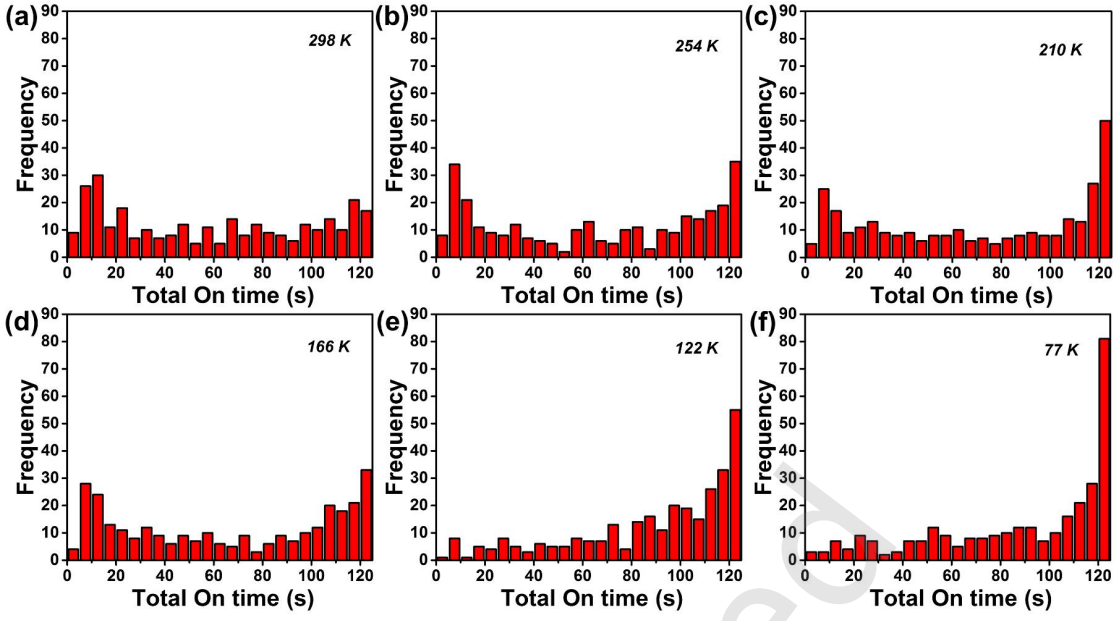


Figure S5. Distribution of the total on-time individual R-CDs under different temperature.

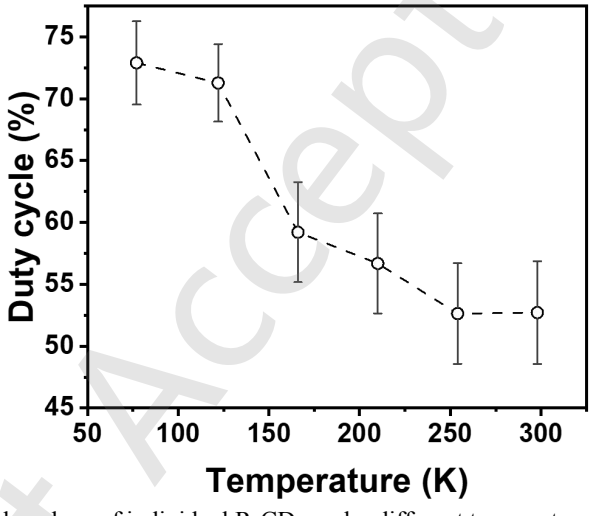


Figure S6. Distribution of the duty cycle values of individual R-CDs under different temperature.

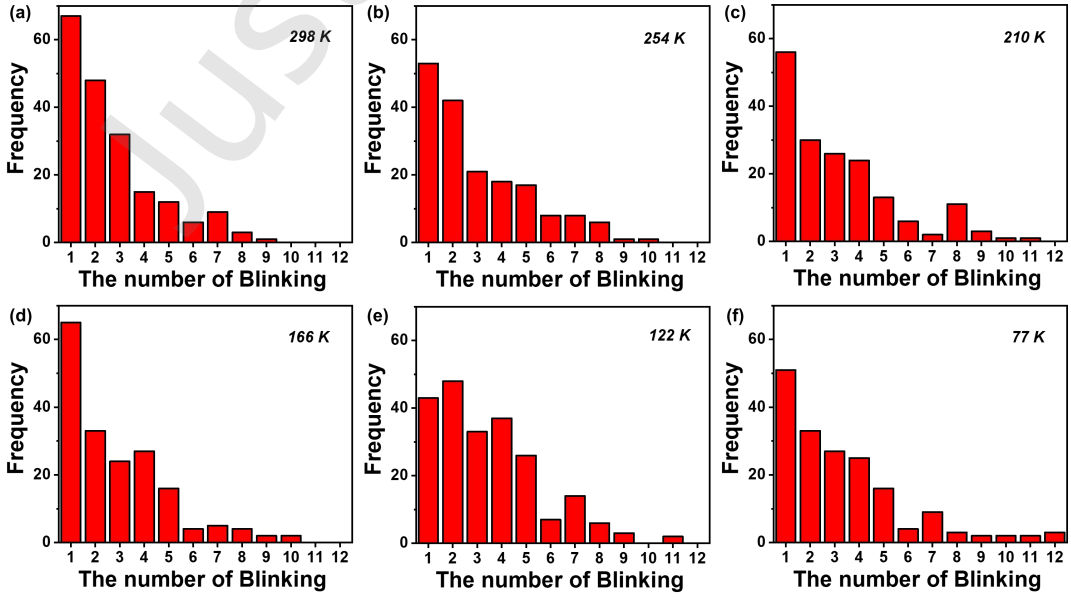


Figure S7. The variation in blinking frequency with temperature.

Just Accepted